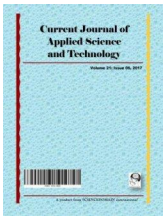

Current Journal of Applied Science and Technology

30(4): 1-12, 2018; Article no.CJAST.44341
ISSN: 2457-1024
(Past name: British Journal of Applied Science & Technology, Past ISSN: 2231-0843, NLM ID: 101664541)

Wave Energy Impact on Benin's Coastline Dynamics, Gulf of Guinea

Guy Hervé Hounguè[1,2*], Basile Bruno Kounouhéwa[1,2,3], Bernard Noukpo Tokpohozin[2,4], Mathias Adjimon Houékpohéha[2,4], Vianou Irénée Madogni[1,2*] and Rafael Almar[5]

[1]Département de Physique (FAST) et Formation Doctorale Sciences des Matériaux (FDSM), Université d'Abomey-Calavi, Bénin.
[2]Laboratoire de Physique du Rayonnement (LPR), FAST-UAC, 01 BP 526 Cotonou, Bénin.
[3]Institut des Recherches Industrielles, Technologiques et en Sciences Exactes (IRITESE/CBRSI), Bénin.
[4]Institut de Mathématique et de Sciences Physiques (IMSP), Dangbo, Bénin.
[5]LEGOS (CNRS/CNES/IRD/Université de Toulouse), France.

Authors' contributions

This work was carried out in collaboration between all authors. All authors read and approved the final manuscript.

Article Information

DOI: 10.9734/CJAST/2018/44341
Editor(s):
(1) Dr. Vyacheslav O. Vakhnenko, Professor, Division of Geodynamics of Explosion, Subbotin Institute of Geophysics, National Academy of Sciences of Ukrainian, Ukraine.
Reviewers:
(1) Fábio Henrique Portella Corrêa de Oliveira, Universidade Federal Rural de Pernambuco, Brazil.
(2) Tunde Aderinto, Texas A&M University, USA.
(3) Beata Messyasz, Adam Mickiewicz University in Poznan, Poland.
Complete Peer review History: http://www.sciencedomain.org/review-history/27177

Original Research Article

Received 02 August 2018
Accepted 08 October 2018
Published 13 November 2018

ABSTRACT

Most of the shorelines around the world are affected by the phenomenon of coastal erosion, especially the Benin's coastline.
We investigated the parameters (significant height, peak period and peak direction) and wave energy potential offshore Benin from ECMWF ERAI reanalysis. ERAI data have been adjusted with in situ data coming from the buoy installed off Autonomous Port of Cotonou (Benin) over a period of 14 years. Next, statistical analysis has been used to establish the link between wave energy and Benin's coastline dynamics. Wave energy assessment has been carried using the empirical formula for medium water depths consideration (equation (10)).
The results show that in Benin's coastal area, wave energy potential is moderate and available (Hs $\simeq$1.36m, Tp$\simeq$ 9.6 s and P $\simeq$15.56kW.m^{-1}). At seasonal scale, wave energy density P and coastline

**Corresponding authors: E-mail: hguyherv@gmail.com, madognimadogni@gmail.com;*

displacement are strongly linked ($R^2 = 0.9$).
Wave energy exploitation will contribute to energy independence and will play a crucial role in mitigating of coastal erosion effects and consequently in the protection of the country's coastline.

Keywords: Coastal erosion; Benin coastline; wave energy; coastal protection.

1. INTRODUCTION

More than 70% of beaches are eroding [1], and beach erosion is a global problem [2]. Intensification of urban development results from expanding coastal use by human populations [3], and almost every beach on every coastline is threatened by human activities [4]. Benin, a coastal country in Gulf of Guinea, has not been spared by the phenomenon of coastal erosion. Erosion observed on Benin's coastline is accentuated by the human installations: port with dykes blocking the coastal drift, urbanization with fixing of the dune cord, construction of dams upstream of the rivers, thus reducing sediment inputs. Indeed, the sedimentary equilibrium of this coastline is precarious, it depends on the dynamics of coastal drift, one of the largest in the world (≃500 000 m^3/year) [5], which is put into motion by swells generated in the South Atlantic. As a result, the coastline is experiencing a very significant decline, ranging from 2 to more than 30m per year from Côte d'Ivoire to Nigeria [6-9]. The geographical location of the country, offers the possibility of exploiting wave energy, which could contribute to the mitigation of coastal erosion observed. Indeed, there are currently, several wave energy recovery devices that play an active role in coastal protection. These recovery devices are particularly interesting since they partially absorb waves in producing electricity and may thus reduce the wave energy incident on the littoral [10]. Recent studies [10-13] showed that nearshore currents, which are the main factor in driving the coastline dynamics, are sometimes even more sensitive than the waves to the nearshore energy extraction. This is explained by the fact that the wave farms induce relevant changes; not only to the wave heights but also to the wave directions [14]. Wave energy in Benin coastal area, if available, will contribute to the country's energy dependence. Although very crucial, the characteristics (minimum, average, maximum, inter-annual and seasonal variability) of the wave energy resource in Benin's coastal zone are poorly known.

In this paper, wave energy has been characterized and analysed using European Center for Medium-Range Weather Forecasts (ECMWF) reanalysis (ERA-Interim) datasets adjusted with in situ data coming from the buoy installed off Autonomous Port of Cotonou (Benin) over a period of 14 years. Next, the link between wave energy and Benin coastline dynamics has been investigated using statistical analysis.

2. MATERIALS AND METHODS

2.1 Study Area

Benin's coastline, 125 km long, is located between the longitudes E1°5 and 2°5E and the latitudes 5°N and 6°N and facing South Atlantic Ocean (Fig. 1a). It is an open environment exposed to long swell waves. It is an environment dominated by the influence of waves of moderate energy (mean significant wave height Hs = 1.36 m, mean peak period Tp = 9.4 s) coming from mid-to high latitudes (45–60°) in the South Atlantic as well as to locally generated short-waves in the tropical band (latitude 6°N to longitude 15°S) with an S-SW incidence (incidence on the coast between 4 and 10°) [5,15].

2.2 Data sets

2.2.1 Buoy data

Wave parameter data from the buoy deployed offshore about 6 Km from the Autonomous port of Cotonou and more than 15m deep at the coordinates (latitude 6°18'49N, longitude 2°28'46E) are used (Fig.1c). Waves parameters significant wave height (Hs), peak period (Tp) and peak direction (Dp) are recorded every 30 min (48 daily data). The buoy data used here cover the period from December 2015 to October 2016.

2.2.2 ERAI reanalysis

The simulations used were provided by ERA-Interim (1.5°x1.5°) of the European Center for Medium-Range Weather Forecasting (ECMWF). ERA datasets has always been used and validated in the Gulf of Guinea [5,15]. Wave parameters used are (Hs, Tp and Dp). These parameters are stored four times a day (temporal resolution: 6h). The outputs used are calculated at the point (latitude 6°0 N; longitude 3°0'E). ERAI datasets cover the period 2003-2016.

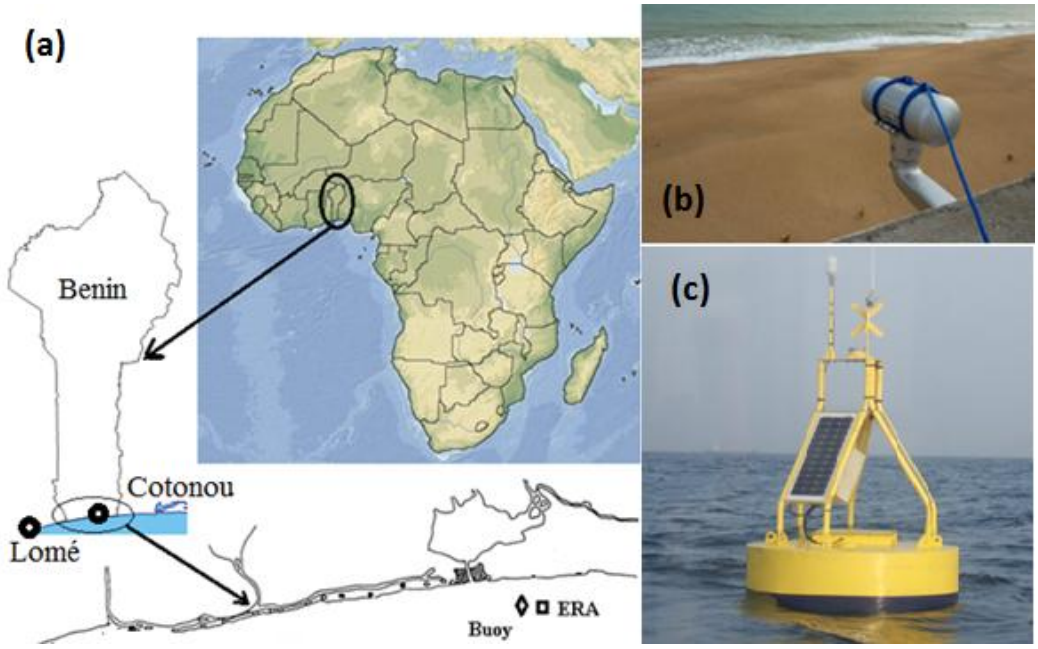

Fig. 1. Sketch of study area (Benin, Gulf of Guinea) a.) with location of ERA and Buoy; b.) camera system and c.) Oceanographic buoy

2.2.3 The camera system

In February 2013, a low-cost video system was installed on the top of a tower of the Navy Forces of Benin in Grand Popo, about 70 m from the shoreline [16]. The system was composed of a VIVOTEK IP 7361 camera (1600-728 pixels), which collected data continuously at 2 Hz (Fig. 1b). Twenty ground control points were taken with GPS to process image geo-rectification [17], by applying the method of direct linear transformation [18]. See [16,19-21] for more description. Data used here are about shoreline position.

2.3 Data validation

A comparison between ERAI model outputs and the buoy data indicates an over-estimation of the extremes at the reanalysis with respect to the buoy data. Although the mean values are well described. ERA reanalysis model reproduces the large swells (Hs > 1m) but misses the small ones (Hs < 1m). The correlation between the buoy data and the model outputs ($R^2 = 0.80$ for Hs, $R^2 = 0.49$ for Tp) made it possible to consider an adjustment between the significant heights Hs, peak period Tp observed (buoy) and estimated (ERAI). The linear adjustment is written by:

$$\begin{cases} \mathrm{H_{sb}} = 1.03 * \mathrm{H_{sm}} - 0.10 \\ \mathrm{T_{pb}} = 0.55 * \mathrm{T_{pm}} + 0.45 \end{cases} \quad (1)$$

where H_{sb} and T_{pb} represent respectively the significant height and the peak period of waves measured by the buoy and H_{sm}, T_{pm} derived from ERAI. This adjustment is used for the characterization of wave parameters and consequently average energy density in Benin coastline area.

2.4 Theory

2.4.1 Wave energy density estimation

Wave power density is a very important parameter for wave energy assessment, which has been calculated in recent studies by integrating model spectra based on numerical wave models [22]. In shallow or medium water depths, the nearshore effects must be considered when calculating this parameter, including refraction, shoaling, bottom dissipation and sheltering by the coastline or adjacent islands [23]. Hence, in shallow water, the wave power P per unit of crest length (kW.m^{-1}) can be obtained using the following expression [24]:

$$\mathrm{P} = \frac{1}{\mathrm{T}} \int_0^{\mathrm{T}} \int_{-\mathrm{h}}^{0} (\mathrm{p} + \rho \mathrm{gz}) \mathrm{udtdz} \quad (2)$$

where t: the time (s); T: wave period (s) and z: water depth (m).

The integral of equation (2) over the wave period and the water depth conduced to P. Therefore, P can be calculated using [25]:

$$\mathrm{P} = \overline{\mathrm{E}}\mathrm{C_g} \quad (3)$$

where C_g denotes wave group velocity and $\bar{E}$(J/m^2), the wave energy density which ones can respectively be express as follows;

$$\mathrm{C_g} = \frac{1}{2}\left[1 + \frac{2\mathrm{kh}}{\sinh(2\mathrm{kh})}\right] \times \mathrm{C} \quad (4)$$

$$\overline{\mathrm{E}} = \frac{1}{16}\rho \mathrm{g} \mathrm{H_s^2} \quad (5)$$

where H_s denotes significant wave height; ρ the density of seawater (assumed to be 1025 kg.m^3) and g, the gravitational acceleration (assumed to be 9.81N.kg^{-1}).

The wave number k (m^{-1}) as a function of λ (wavelength) (m) is giving by:

$$k = \frac{2\pi}{\lambda} \quad (6)$$

The phase velocity C can be expressed as follows;

$$C = \frac{\lambda}{T} = \left(\frac{g}{k}\tanh(kh)\right)^{\frac{1}{2}} \quad (7)$$

In the deep water ($\frac{\mathrm{h}}{\lambda} \geq \frac{1}{2}$; $\left[1 + \frac{2\mathrm{kh}}{\sinh(2\mathrm{kh})}\right] = 1$ and $\tanh \mathrm{kh} \simeq 1$) were included in equation (3) and rearranged conduced to [22]:

$$\mathrm{P} = \frac{\rho\, \mathrm{g}^2}{64\, \pi} \mathrm{H_s^2 T_e} \quad (8)$$

Where $\mathrm{T_e}$ is the energy period.

In shallow or medium water depths, the nearshore effects must be taken account when calculating the wave power density, including refraction, shoaling, bottom dissipation and sheltering by the coastline or adjacent islands [23]. Indeed, in the shallow water, ($h/\lambda < 1/20$; $\left[1 + \frac{2kh}{\sinh(2kh)}\right] = 2$ and $\tanh(\mathrm{kh}) = \frac{2\pi \mathrm{h}}{\lambda}$)

Equation (3) can then be rewritten:

$$\mathrm{P} = \frac{1}{16}\rho \mathrm{g} \mathrm{H_s^2}\sqrt{\mathrm{gh}} \quad (9)$$

For medium water depths, ($1/20 < h/\lambda < 1/2$), shallow water correction must be considered and P can be calculated as:

$$\mathrm{P} = \overline{\mathrm{E}}\left(\frac{\mathrm{g\, T_e}}{2\,\pi}(\tanh(\mathrm{kh}))^{\frac{1}{2}}\right) * \left[\frac{1}{2} * \left(1 + \frac{2\,\mathrm{k\,h}}{\sinh(2\mathrm{kh})}\right)\right] \quad (10)$$

With

$$\lambda = \frac{\mathrm{g}}{2\pi}\mathrm{T_e^2} \quad (11)$$

T_e is computed as a function of spectral moments [26-27]:

$$\mathrm{T_e} = \frac{\mathrm{m_{-1}}}{\mathrm{m_0}} \quad (12)$$

Another approach when T_p is known, the energy period can be assumed as [26-28]:

$$\mathrm{T_e} \simeq \alpha \mathrm{T_p} \quad (13)$$

where α is a coefficient whose value depends on the shape of the wave spectrum (e.g. 0.86 for a Pierson-Moskowitz spectrum). More conservative assumption of α has been adopted ($\alpha = 0.90$ or $T_e \simeq 0.9T_p$) [27]. This assumption introduces uncertainty in the resulting wave power. However, the errors in the period are less significant than errors in wave height since P is proportional to T_e and to the square of the H_s [29].

The buoy ALIZE, is deployed offshore off Benin's coastline about 6 Km at 15 m depth corresponding to medium water. Then, we use in this work, the equation (10) for wave power calculation and we assumed that T_e = T_p.

2.4.2 Longshore sediment transport rate (LST)

Several empirical formulas are used for LST's calculating. In this work formula proposed by Kamphuis [30] has been used. This empirical formula (equation 14) predicted the longshore sediment transport rates much more accurately [31]. Longshore sediment transport formulae require as input the breaking wave parameters, but global wave hindcasts only provide deepwater characteristics [5].

$$\mathrm{I} = 2.33 * \mathrm{H_{sb}^2 T_p^{1.5}} \delta^{0.75} \mathrm{d}^{-0.25} \sin^{0.6}(2\alpha_\mathrm{b}) \quad (14)$$

where I denotes the longshore transport rate in (underwater) kilograms per second (kg/s), H_{sb} the breaking wave height, α_b the local breaking wave angle, Tp is the peak period, δ the beach

slope inducing the breaking (i.e. the ratio of wave depth at breaker line and the distance from the still water beach line to the beaker line) and $d = d_{50}$ the mean sediment grain size; d is here equal to 0.60 mm based on Anthony and Blivi [32]. The value 2.33 is the dimensional coefficient related to the SI system assuming salt water (1025 kg/m^3). Although using a nested numerical model (e.g. SWAN or WW3) to propagate waves from deep water to the break point would have been an ideal option for a short-term study, because of the difficulties presented by the spatio-temporal scales of this study, we have used here the empirical breaking wave predictor proposed by Larson et al. [33] and tested by Almar et al. [5]. The empirical breaking wave predictor formula has been proposed, to estimate H_{sb} which directly provides breaking wave height H_{sb} and angle α_b, given deepwater wave heighth_0, period T and direction α_0 :

$$H_{sb} = \lambda \frac{c^2}{g} \quad (15)$$

$$\alpha_b = a\sin(\sin(\alpha_0)\sqrt{\lambda}) \quad (16)$$

where λ denotes a correction factor defined as :

$$\lambda = \Delta\lambda_\alpha \quad (17)$$

Where

$$\Delta = 1 + 0.1649\zeta + 0.5948\zeta^2 - 1.6787\zeta^3 + 2.8573\zeta^4$$

$$\zeta = \lambda_\alpha \sin\theta^2$$

$$\lambda_\alpha = [\cos(\alpha_0)/\theta]^{\frac{2}{5}} \text{ and}$$

$$\theta = \left(\frac{C}{\sqrt{gH}}\right)^4 \left(\frac{C}{C_g}\right)\gamma^2$$

with γ, the constant breaker index defined by equation (18) as follow [34] :

$$\gamma = \frac{H_{sb}}{\alpha_b} = 0.78 \quad (18)$$

The wave phase velocity C and group velocity C_g can be obtained by equations (4) and (7).

3. RESULTS AND DISCUSSION

3.1 Sea-wave Instantaneous Characterisation

Fig. 2a shows average scatter sea-wave regime in terms of Hs and Tp and Fig. 2b indicates the compass rose of wave directions (Dir-Hs) for the 10 months and half period of buoy dataset. Fig. 2 shows that in Benin coastal area, the significant wave height can reach more than 2,5 m. The wave periods range from 4 to 14 s and mean wave directions from 180° to 227° and 165° to 180° (S-SW clockwise). In general, the waves have significant heights between 0.5 and 2.53 m from the south-west quadrant, i.e., 190° to 235°. The most frequent wave periods are between 5.2 to 10 s. The interval 6-9 s has the most occurrences. It should be noted that several wave trains are concomitant in the Gulf of Guinea even but the peak energy is dominated by long swells of the south-west. This is due to the fact that the coast is quite far from the swelling generation zone to be affected by local and remote waves, which facilitates the coexistence of multiple wave generation zones [5].

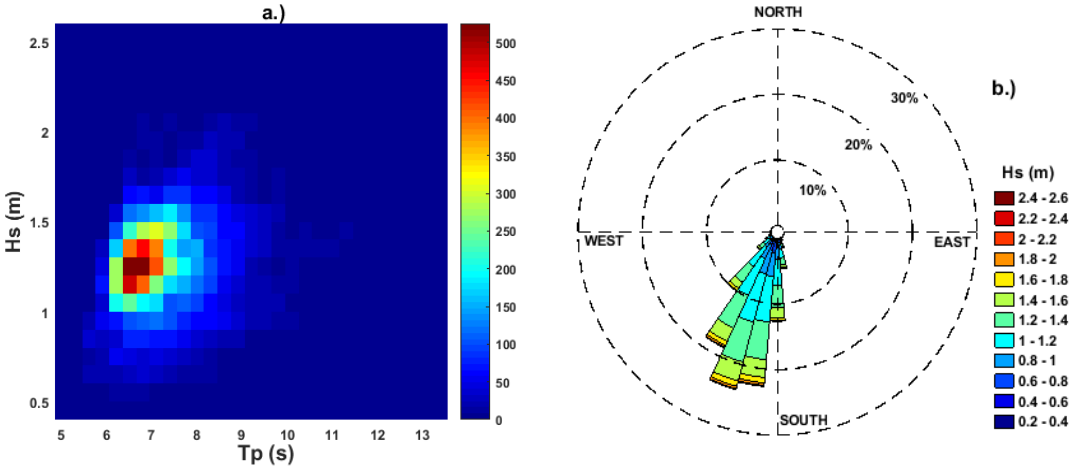

Fig. 2. Wave scatter diagram (a) and compass rose of wave directions (b) for the period 2015–2016 in Benin coastal area from buoy data sets

3.2 Sea-wave Long Term Characterization

3.2.1 Wave parameters instantaneous variability

The equations (1) are used to estimate wave parameters for long term wave consideration and then for wave energy assessment. Fig. 3a indicates average scatter sea-wave regime in terms of Hs and Tp and Fig. 3b the compass rose of wave directions Dir-Hs for the 14-years period of ERAI reanalysis dataset. Hs averaged occurrences are found between 0.5 and 2.1m (with the most frequent values from 1 to 2 m), associated with mean wave directions from the South/South-West (182°–210°). The most frequent for wave periods (Tp) are between 6.5 to 13.5 s and 1 to 2.5m for significant wave height (Hs). The interval 7–12 s has the most occurrences for wave period. A statistical study shows that 85.47 percent of Tp was greater than 8 s indicating the predominance of the swell.

3.2.2 Wave parameters seasonal variability

Fig. 4 shows the averaged sea-wave regime in terms of Hs and Tp. At seasonal scale the maximum values of Hs are observed from May to September ranged from 1.19 to 1.68 m averaged of 1.44m with peak values in June, July and August. The figure indicates an increasing tendency of Hs from January to July and decreasing tendency until December. Wave peak period ranging from 8.54 to 9.55s averaged of 9.17s. The seasonality observed is related to wind variability in the Atlantic Ocean. In fact, the winds generated in the South Atlantic maximum

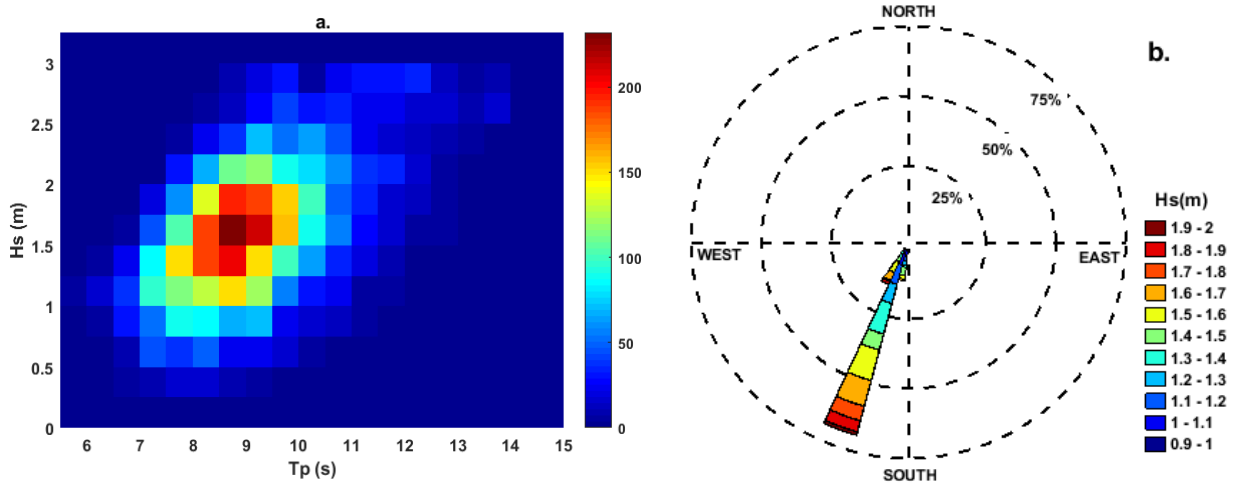

Fig. 3. Wave scatter diagram (a) and compass rose of wave directions (b) for the period 2003–2016 in Benin coastal area from ERAI data sets adjusted by buoy data

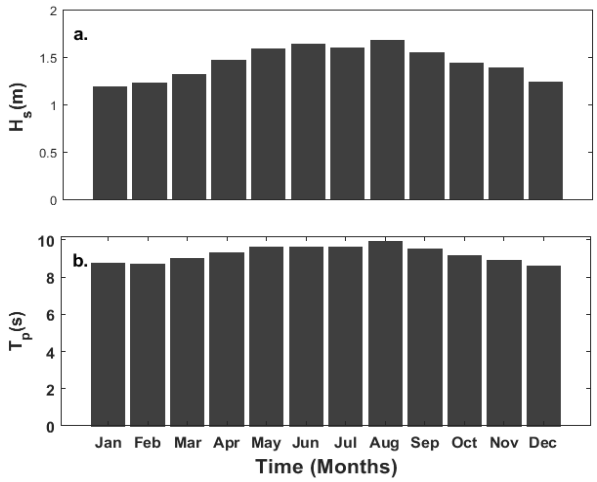

Fig. 4. Averaged Hs (a) and Tp (b) wave regime in Benin's coastal area

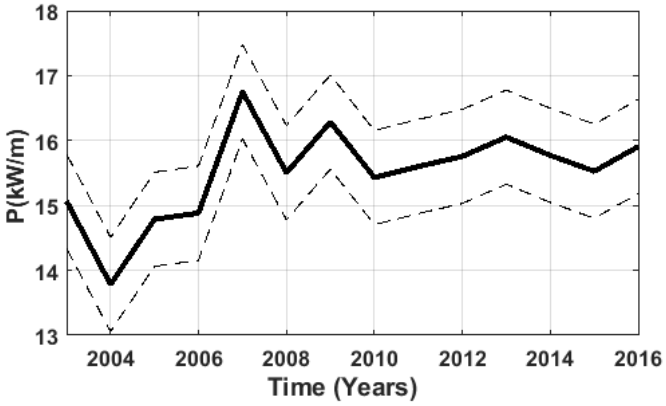

Fig. 5. Annual averaged wave power (14 years). The dashed lines indicate the standard deviation of annual wave power

in July, increase from January to July and then decrease until December. The seasonality observed is related to wind variability in the Atlantic Ocean. In fact, the winds generated in the South Atlantic maximum in July, increase from January to July and then decrease until December [35-36].

3.3 Wave Energy Potential Analysis in Benin Coastal Area

3.3.1 Wave energy inter-annual variability

Fig. 5 indicates wave annual power variability P, from 2002 to 2016 using equation (9) when all types of waves have been taken into account. The figure shows an increasing tendency of wave power ranging from 13.78 to 16.78 kW.m^{-1} averaged of 15.56 kW.m^{-1} with (std=0.72). The majority of wave power averaged (Pav) occurrences are found in the interval of 14.5 and 17 kW.m^{-1} (with the most frequent values from 15 to 16.5 kW.m^{-1}). This trend is related to this of the significant height in the Gulf of Guinea. Indeed, Abessolo et al. [21] and Xorse [36] observed an increasing tendency of significant wave height respectively in Ghana and Benin coastal areas. In the sub-region, there is no knowledge of work in this area. But further south, along the South African coast, the average annual wave power available varied from 33 to 41kW.m^{-1}, [37], higher than that found in this work. Referring to the global average wave energy map [38], our results seem to overestimate the values contained therein. Indeed, according to this map, energy available to Beninese coastal area is between 5 and 12kw.m^{-1}. It is important to note that this map was carried out with deep water consideration which is not the case of this study where the energy is assessed with medium water consideration.

3.3.2 Inter-annual statistic of wave energy density

Inter-annual characteristics of annual wave energy deduced from Fig. 5 have been mentioned in Table 1.

Table 1. Inter-annual characteristics of wave energy off Cotonou from 2003 to 2016 and its standard deviation (σ)

Min (kW.m^{-1})	Mean (kW.m^{-1})	Max (kW.m^{-1})	σ
13.78	15.57	16.78	0.72

3.3.3 Wave Seasonal variability

The energy in Benin marine area is strongly influenced by seasonal fluctuations. Fig. 6a indicates wave power's seasonal variability (P) from 2003 to 2016 using equation (9) when all types of waves have been taken into account. The figure shows an increasing tendency of wave power with (std=2.9) from January to August and decreasing tendency until December with values rangind from 9.64 to 21.82 kW.m^{-1} averaged of 15.76 kW.m^{-1}. The result can be attributed to wave significant height in Gulf of Guinea (Fig. 5a) [15]. The low values were observed from December to February where the power is less than 15kW.m^{-1} and the maximum values from March to November where the power is between 15-21.82 kW.m^{-1}. Pronounced seasonal variations in the wave energy are present in this area (Fig. 6b). Fig. 6b, indicates

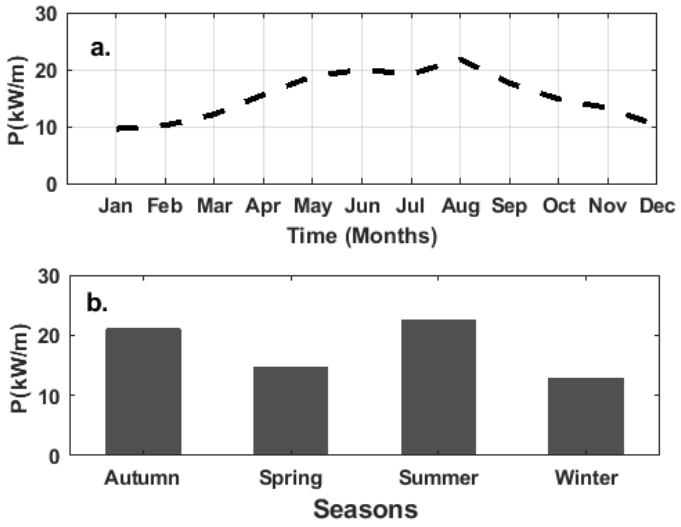

Fig. 6. Average wave energy density, (a) monthly and (b) for each season of the year in Benin marine area

the assessment of wave energy for the different seasons of year. The wave energy is larger in summer and autumn (20-21.85 $kW.m^{-1}$) than at in spring and winter (12.75-14.95 $kW.m^{-1}$); so the wave energy exploitation is mainly in autumn and winter. This variability is similar to the global seasonal distribution of average wave power [29]. Indeed, wave energy average estimated by the global distribution is less than 11k $W.m^{-1}$in January and between 11-22 $kW.m^{-1}$ in July.

3.3.4 Seasonal statistic of wave energy density

Seasonal characteristics of annual wave energy deduced from Fig. 6 have been mentioned in Table 2.

Table 2. Inter-annual characteristics of wave energy off Cotonou from 2003 to 2016 and its Standard deviation (σ)

Min ($kW.m^{-1}$)	Mean ($kW.m^{-1}$)	Max ($kW.m^{1}$)	σ
9.64	15.76	21.85	2.67

3.4 Interannual Variability of Longshore Sediment Transport (LST)

Wave parameters characteristics on Benin's coastline (incidence ≈9.4 °) induce a longshore current that generates a littoral drift. This drift observed along the coasts of the Gulf of Guinea countries, one of the largest in the world has been estimated in this work using formula proposed by Kamphuis [30], the breaking parameters coming from the empirical breaking wave predictor proposed by Larson et al. [33]. Fig. 7 indicates inter-annual variability of the longshore sediment flux (LST) estimated from formula 14. This figure shows a significant upward trend of LST with values ranging from 4.56 $x10^5$ to $5.71x10^5$ with an average of $5.15x10^5$ m^3/year (std = $3.12x10^4$) directly related to the observed increase in significant wave height in the study area (Gulf of Guinea). Our results are in agreement with those found by Almar et al. [5]. Indeed, using the model developed by Kaczmarek et al. [39], the authors found a longshore sediment flux averaged of $\simeq 5x10^5 m^3$/year on Beninese coast. A little further west, on Ghanaian's coast for example, the longshore sediment flux was estimated at $7.65x10^5 m^3$/year as a result of the large waves on these exposed open ocean coasts [40]. Further north, [41] using the same theory as [5], found results overestimating those found in our study($\simeq 7x10^5$ m^3/year) on Senegalese coast.

3.5 Shoreline Position and Offshore Wave Variability

Wave parameters characteristics on Benin's coastline (wave incidence ≃ 9.4° on average) show the involvement of the swell in the phenomenon of coastal erosion. Wave impact on shoreline evolution was investigated using seasonal variability analysis of shoreline position and the one of wave energy. Fig. 8 shows seasonal wave energy and shoreline position

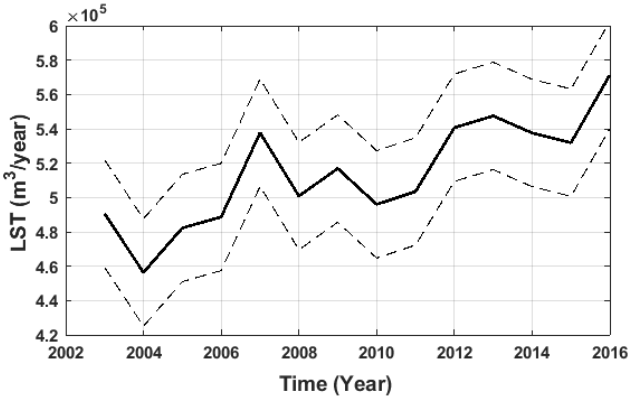

Fig. 7. Inter-annual variability of longshore sediment transport using offshore wave characteristics. The dashed lines indicate the standard deviation of LST

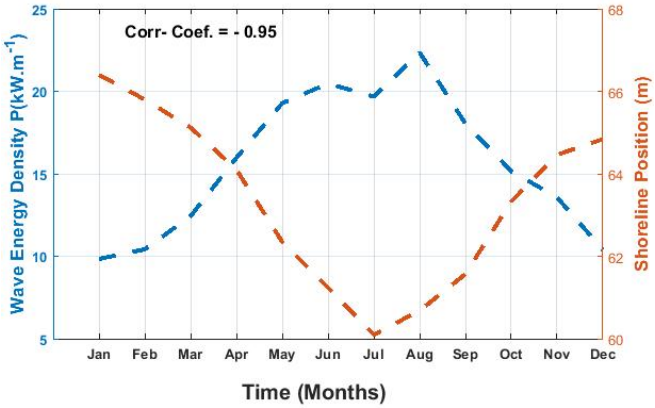

Fig. 8. Seasonal cycle comparison between shoreline position (red) and offshore wave energy (blue)

time series. Seasonal cycle of the shoreline position (red curve) presented two main different phases, the erosive phase (January-July) and accretive phase (July to December). The figure indicates that for the first phase, wave energy increases from 10 to 20 kW/m but the shoreline has moved from the position 66.70 to 60 m, which shows an average sea advance of 6 m on the coast. For the second phase, wave energy decreases from 22 to 10.3 kW/m but shoreline position increase from 60 to 65 m showing an accretion during this phase. This shows that at the seasonal scale, the dynamics of Benin's coastline is strongly influenced by wave energy. Statistical analysis shows that wave energy density and shoreline position are negatively correlated (Correlation $\text{coefficient} = -0.95$). Our results are in agreement with those mentioned in Senechal et al. [42] who have shown that periods of accretion and erosion are generally associated with low and high energy wave conditions respectively, but they also exhibit strong site-specific variations. In addition to wave energy effects on Benin's coastline dynamics, those related to climate change (rising sea level and intensifying scenarios of recent storms) must be taken into account. Indeed, for many coastal regions, both sea-level rise and changes in the storm-wave climate would result in coastal erosion and an increased frequency with a high intensity of coastal flooding [21]. Moreover, in the case of an increase in the effective sea level, the coastline would be reduced according to the general scheme of [43].

4. CONCLUSION

Wave energy potential in Benin coastal area has been characterized and analysed using fourteen years ERA reanalysis of European Center for Medium-Range Weather Forecasts (ECMWF) wave data sets adjusted with buoy data deployed offshore about 6 Km from the Autonomous port of Cotonou (Benin) and more than 15m deep at

the coordinates (2°28'46E, 6°18'49N). After, the link between wave energy and coastline has been investigated.

The results indicate that wave energy in Benin coastal area is moderate and available (Hs ≃ 1.36 m, Tp≃9.6s and P≃16.62 kW.m^{-1} per wave front). Wave energy is influenced by seasonal variability related to wave parameters (Hs and Tp) in the study area. At seasonal scale, wave energy density and shoreline position are strongly linked ($R^2 = 0.9$).

Given the link between wave energy variability and coastline evolution, wave energy exploitation will help Benin country to improve its energy autonomy and consequently contribute to the mitigation of coastal erosion phenomenon observed this coast.

ACKNOWLEDGEMENTS

The authors thank Benin Center for Scientific Research and Innovation (CBRSI) for accompanying this research work.

We acknowledge use of the ECMWF ERA Interim dataset (www.ECMWF.Int/research/Era).

COMPETING INTERESTS

Authors have declared that no competing interests exist.

REFERENCES

1. Bird CF. Beach management (Coastal Morphology and Research). Wiley, Chichester; 1996.
2. Komar PD, Inman DL. Longshore sand transport on beaches. Journal of Geophysical Research. 1970;75(30): 5914–5927.
3. Nordstrom KF. Beaches and dunes on developed coasts. Cambridge University Press, UK; 2000.
4. Defeo O, McLachlan A, Schoeman DS, Schlacher TA, Dugan J, Jones A, Lastra M, Scapini F. Threats to sandy beach ecosystems: A review. Estuarine, Coastal and Shelf Science. 2009;81:1–12.
5. Almar R, Kestenare E, Reyns J. Response of the Bight of Benin (Gulf of Guinea, West Africa) coastline to anthropogenic and natural forcing, Part1: Wave climate variability and impacts on the longshore sediment transport. Continental Shelf Research. 2015;110:48-59.
6. Ibe AC, Awosika LF. Sea level rise impact on African coastal zone. A change in the weather: African perspectives on climate change. In Omide S H, Juma C, Eds. 105-12. Nairobi, Kenya, African center for technology studies. No paginated; 1991.
7. Rossi G. L'Erosion du littoral dans le Golfe du Bénin: un exemple de perturbation d'un équilibre morphodynamique. Zeitschriftfür Geomorphologie: Supplementbände. 1991; 73:139-165.
8. Kaki C, Laibi RA, Oyede, LM. Evolution of beninese coastline from 1963 to 2005: Causes and consequences. British Journal of Environment and Climate Change. 2011;1:216–231.
9. Dossou K M R, Glehouenou-Dossou B. The vulnerability to climate change of Cotonou (Benin). Environment and Urbanization. 2007;19(1): 65-79.
10. Mendoza E, Silva R, Zanuttigh B, Angelelli E, Lykke A T, Martinelli L, Nørgaard JQH, Ruol P. Beach response to wave energy converter farms acting as coastal defence. Coastal Engineering. 2014;87:97–111.
11. Iglesias G, Carballo R. Wave farm impact: The role of farm-to-coast distance. Renewable Energy. 2014;69:375–385.
12. Chang G, Ruehl K, Jones CA, Roberts J, Chartrand C. Numerical modeling of the effects of wave energy converter characteristics on nearshore wave conditions. Renewable Energy. 2016;89: 636-648.
13. Zanuttigh B, Angelelli E. Experimental investigation of floating wave energy converters for coastal protection purpose. Coastal Engineering. 2013;80:148–159.
14. Rusu E. Evaluation of the Wave Energy Conversion Efficiency in Various Coastal Environments. Energies. 2014;7:4002-4018
15. Laibi R, Anthony E, Almar R, Castelle B, Senechal N. Alongshore drift cell development on the human-impacted Bight of Benin sand barrier coast, West Africa. In Proceedings 13th International Coastal Symposium (Durban, South Africa), Journal of Coastal Research. 2014;SI 70: 78-83.
16. Almar R, Michallet H, Cienfuegos R, Bonneton P, Ruessink BG, Tissier M. On the use of the random transform in studying nearshore wave dynamics. Coastal Engineering. 2014;92:24–30

17. Angnuureng D B, Almar R, Addo K A, Castelle B, Senechal N, Laryea S W, Wiafe G. Video observation of waves and shoreline change on the Microtidal James Town Beach in Ghana. Proceedings of the 14th International Coastal Symposium, Sydney. Journal of Coastal Research. 2016;SI 75:1022–1026.
18. Holland K T, Holman R A, Lippmann T C. Practical use of video imagery in near-shore oceanographic field studies. IEEE Journal of Oceanic Engineering. 1997; 22: 81–92.
19. Almar R, Ranasinghe R, Senechal N, Bonneton P, Roelvink D, Bryan K R, Marieu V, Parisot J-P. Video-based detection of shorelines at Complex Meso–Macro Tidal Beaches Journal of Coastal Research. 2012;28(5):1040–1048.
20. Almar R, Cienfuegos R, Catalán PA, Michallet H, Castelle B, Bonneton P, Marieu V. A new breaking wave height direct estimator from video imagery. Coastal Engineering. 2012;61:42–48.
21. Abessolo OG, Bonou F, Tomety FS, du Penhoat Y, Perret C, Degbe CGE, Almar R. Beach response to wave forcing from event to inter-annual time scales at grand popo, Benin (Gulf of Guinea). Water. 2017;9:1-13.
22. Wan Y, Zhang J, Mrng J, Wang J. A wave energy resource assessment in the China's seas based on multi-satellite merged radar altimeter data. Acta Oceanologica Sinica. 2015;34(3):115–124.
23. Iglesias G, López M, Carballo R, Castro A, Fraguela JA, Frigaard P. Wave energy potential in Galicia (NW Spain). Renewable Energy. 2009;34(11):2323–2333.
24. Wang C, Lu W. Analysis methods and reserves evaluation of ocean energy resources (in Chinese). Beijing: China Ocean Press. 2009;61–62.
25. Mirzaei A, Tangang F, Juneng L. Wave energy potential assessment in the central and southern regions of the South China Sea. Renewable Energy. 2015;80:454-470.
26. Yaakob O, Hashim FE, Omar KM, Md Din AH, Koh KK. Satellite-based wave data and wave energy resource assessment for South China Sea. Renewable Energy. 2016;88:359-371.
27. Pastor J, Liu Y. Wave energy resource analysis for use in wave energy conversion, J. Journal of Offshore Mechanics and Arctic Engineering. 2015;13:1-9.
28. Sierra J P, Martín C, Mösso C, Mestres M, Jebbad R. Wave energy potential along the Atlantic coast of Morocco. Renewable Energy. 2016;96:20-32.
29. Cornett V. A global wave energy resource assessment. In: International offshore and polar engineering conference (ISOPE). 2008;1:318–326.
30. Kamphuis JW. Alongshore sediment transport rate. J. Waterway Port Coastal Ocean Engineering. 1991;117(6):624–640.
31. Wang P, Ebersole BA, Smith ER. Longshore sand transport-initial results from the large-scale sediment transport facility. US Army Engineer Research and Development Center, Vicksburg, Mississippi (peer-reviewed). 2002; ERDC/CHL CHETN-II-46.
32. Anthony EJ, Blivi AB. Morpho-sedimentary evolution of a delta-sourced, drift-aligned sand barrier-lagoon complex, western Bight of Benin. Marine Geology. 1999;158: 161–176.
33. Larson M, Hoan LX, Hanson H. A direct formula to compute wave properties at incipient breaking. Journal of Waterway, Port, Coastal, and Ocean Engineering. 2010;136(2):119–122.
34. Battjes JA, Janssen JPFM. Energy loss and setup due to breaking of random waves. In: Proceedings of International Conference on Coastal Engineering, ASCE. 1978;569–587.
35. Laibi R. Dynamique actuelle d'une embouchure fluviale estuarienne à flèche sableuse: la bouche du Roi, Bénin, Golfe de Guinée. Thèse de Doctorat, Universités UAC et ULCO ; 2010. French
36. Xorse TM-S. Impact of wave dynamics on the coast of Ghana. Thesis of University of Ghana; 2013.
37. Joubert JR, Niekerk JL. Recent developments in wave energy along the coast of southern Africa. Proceedings of the 8th European Wave and Tidal Energy. 2009;1096-1100.
38. Mork G, Barstow S, Kabuth A, Pontes AT. Assessing the global wave energy potential. Proceedings of OMAE. 2010;447-454.
39. Kaczmarek LM, Ostrowski R, Pruszak Z, Rozynski G. Selected problems of sediment transport and morphodynamics of a multi-bar nearshore zone. Estuarine,

Coastal and Shelf Science - Journal. 2005;62:415–425.
40. Hayes MO, Michel J, Holmes JM. A Coast for All Seasons: A Naturalist's Guide to the Coast of South Carolina: Pandion Books; 2008.
41. Sadio M, Anthony EJ, Diaw AT, Dussouillez P, Fleury JT, Kane A, Almar R, Kestenare E. Shoreline changes on the wave-influenced Senegal River Delta, West Africa: The Roles of Natural Processes and Human Interventions. 2017;9:1-17.
42. Senechal N, Coco G, Castelle B, Marieu V. Storm impact on the seasonal shoreline dynamics of a meso-to macrotidal open sandy beach (Biscarrosse, France). Geomorphology. 2015;228:448–461.
43. Bruun P. Sea-level rise as a cause of shore erosion. Journal of Waterways and Harbours Division. 1962;88:117-130.

Peer-review history:
The peer review history for this paper can be accessed here:
http://www.sciencedomain.org/review-history/27177